Theor Chim Acta (1996) 94: 247–256

Theoretica Chimica Acta

A comparative QCISD(T), DFT and MCSCF study of the unimolecular, decomposition of the N-chloro-α-glycine anion in gas phase

J.J. Queralt, V.S. Safont, V. Moliner, J. Andrés
Departament de Ciències Experimentals, Universitat Jaume I, Box 242, E-12080 Castelló, Spain

Received May 28, 1996/Final revision received July 29, 1996/Accepted July 30, 1996

Abstract. Stationary points were localized and characterized on potential energy surfaces for the unimolecular decomposition of the anionic form of N-chloro-α-glycine in its singlet and triplet electronic states by means of QCISD(T), DFT and MCSCF methods. The present study predicts that the unimolecular decomposition mechanism takes place in the singlet electronic state through a concerted and slightly asynchronous process and the transition structure has an antiperiplanar conformation. A comparison of the structures for stationary points calculated with different methods yields similar geometries and the components of transition vector are weakly dependent on the computing method.

Key words: Molecular mechanism – N-Chloro-α-glycine – Potential energy surface – Post Hartree–Fock procedures

1 Introduction

Nowadays, the most commonly employed method for the disinfection of drinkable and waste waters is chlorination. In spite of its effective disinfecting properties, it is well established that water chlorination leads to the formation of a wide range of chlorinated by-products, some of which with carcinogenic and/or mutagenic properties [1, 2]. In particular, N-Cl-α-amino acids are found after chlorination of natural waters, decomposing readily to carbon dioxide, chloride ion and different organic products [3] with the following rate-limiting step of the decomposition process [4]:

$$ClR_1N-CR_2R_3-COO^- \longrightarrow R_1N=CR_2R_3 + CO_2 + Cl^- . \qquad (1)$$

Several experimental studies have focused on the stability of N-Cl-α-amino acids in aqueous solution and many different molecular reaction mechanisms have been proposed [4–13], some of them [14] suggesting the participation of the first excited triplet electronic state. On the other hand, previous theoretical studies by our group [15], carried out with semiempirical AM1 and PM3, *ab initio* HF at 4-31G, 6-31G*, 6-311 + G* basis sets and MP2/6-31G* levels of calculation were focused on this reaction and the results can be summarized as follows: (i) an

analysis of the topology of both the singlet and triplet surfaces calculated with all methods demonstrates that the unimolecular process in gas phase takes place in the singlet electronic state and corresponds to a concerted process; (ii) an analysis of the changes of Pauling bond orders [16] of the stationary points shows that the reaction corresponds to a slightly asynchronous process with a transition structure (TS) located in an advanced stage along the reaction path, yielding a product-like character; and (iii) the introduction of the diffuse functions does not appreciably affect the energetic, geometric and mechanistic results.

Our early work [15] used a single reference basis. Since the mechanism under study involves the simultaneous breaking and formation of several bonds, it can be claimed that a single reference wave function is not appropriate for an accurate description of the reaction pathways. Thus, as an extension of the previous works on the reactivity of the N-halo-derivatives, a theoretical study of the unimolecular decomposition of the N-Cl-α-glycine in the gas phase by using multireference wave functions has been carried out. Additionally, the correlation energy was included by means of the variational approach, at the QCISD(T) level, with the aim of confronting the results obtained with the previously reported MP2 study. On the other hand, recent theoretical studies [17–23] have stated that, because they take into account most of the dynamical and non-dynamical correlation effects, the methods based on Density Functional Theory (DFT) are of a quality comparable to the conventional and much more expensive post Hartree–Fock methods. Such statements prompted the inclusion of a method based on DFT in the present study.

In Sect. 2, the model and the computing methods are described. The geometries, energies and activation parameters, the normal modes and the evolution of the bond orders are discussed and analyzed in Sect. 3. A short section of conclusions closes this paper.

2 Model and computational details

The selected model is the N-chloro-α-glycine in its anionic form $ClHN–CH_2–COO^-$ (I). Reactant geometry in the singlet state and numbering of the atoms for the selected model are depicted in Fig. 1.

All calculations were carried out with the GAUSSIAN94 package [24]. Single point quadratic CI calculations [25] with single and double substitutions and a triples, contribution of the energy using the 6-31G* [26] basis set were carried out based on MP2/6-31G* geometries [14]. In spite of dealing with anionic species,

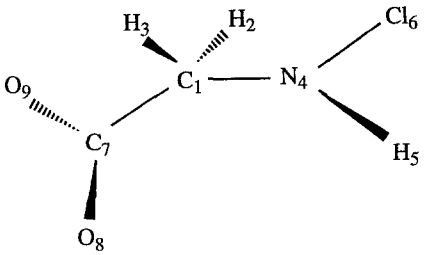

Fig. 1. Numbering of the atoms for the anionic form of N–Cl-α-glycine model

it has been demonstrated in previous calculations [14] that the 6-31G* and 6-311+G* [27–33] basis sets, which include diffuse functions, render similar results within the Hartree–Fock methodology. This is probably due to the fact that the negative charge is delocalized over many centers and diffuse orbitals have been shown to be helpful in describing anions where the negative charge is localized [31]. Nevertheless, these generalizations must be taken with care. Thus, calculations with the 6-311+G* basis set within the DFT [34, 35] which recently received considerable attention [36], have also been performed. The 6-31G* basis set has been chosen for the Multi-Configurational Self-Consistent Field (MCSCF) calculations with the aim of avoiding excessive computational efforts.

For DFT calculations, we used the correlation functional of Lee, Yang, and Parr, which includes both local and non-local terms (LYP) [37, 38] and Becke's three parameter functional (B3) [39] where the non-local correlation is provided by the LYP expression. The calculations were made by using restricted and unrestricted wave functions for the singlet and triplet electronic states, respectively. For the triplet state, we have calculated the natural population of the UHF wave functions. This test shows that very low levels of spin contamination are observed (typical values for $\langle s^2 \rangle$ range between 2.0001 and 2.0088).

The MCSCF methodology has been performed by means of the multiconfiguration SCF wave functions of the complete active space (CAS) SCF class [40]. In CASSCF calculations the assignment of an appropriate active space is decisive for the outcome of the calculations. The active space is not equally appropriate for reactants and TS and it is carefully chosen by an analysis of the orbital population. The occupied and virtual molecular orbitals (MO) of the active spaces are mainly formed by π-atomic orbitals, centered on the heavy atoms (O, C7, C1, N4 and Cl6), which geometrically form σ- and π-bonds. Two combinations have been selected: six electrons and eight orbitals (6, 8), in which the active electrons would correspond to the C1–C7 and N4–Cl6 σ-bonds, and the C1–N4 (in the TSs) π-bond electrons, and eight electrons and eight orbitals (8, 8), in which the decomposition is described by making the correlation of the C1–C7 and N4–Cl6 σ-bonds, and the C7–O and C1–N4 (in the TSs) π-bonds. The distribution among the active orbitals of the corresponding number of active electrons led in each case to CASSCF wave functions formed as a linear combination of a number of doublet spin-adapted configuration state functions which varied from 1177 (6, 8) to 2352 (8, 8). The occupancy of the MOs (from the density matrix) that form the active space for I and TS in the singlet and triplet electronic states has been carefully tested in order to verify a correct correlation between them.

Geometries were optimized using the Berny analytical gradient optimization routines [41, 42] and the TS searching was performed with an "eigenvalue following" optimization method [43, 44]. The nature of a particular stationary point on the PES was confirmed by the number of imaginary frequencies. The harmonic vibrational frequencies of the structures optimized were obtained by diagonalizing the matrix of force constants formed of mass-weighted cartesian coordinates, determined analytically [41, 42].

The frequency calculations also provide data for the calculation of thermodynamic quantities such as the enthalpy and entropy. The raw theoretical harmonic frequencies are scaled by 0.91 [45]. Absolute entropies and temperature corrections were obtained, assuming ideal behaviour, by standard methods [46].

3 Results and discussion

3.1 Geometries

Fully optimized structures for I and TS in its singlet state are reported in Tables 1 and 2, respectively. For I, small differences can be detected between the results obtained with all methods, even if the HF results [15] are included. When DFT methodology is employed, it is important to note that the additional diffuse functions have a very small effect on the geometries. The main differences are found in the N4–Cl6 distances. Small variations are also located on the other variables; for instance, the C1–N4–H5 bond angle changes 2°, the H5–N4–Cl6 bond angle changes 1° and the Cl6–N4–C1–C7 dihedral angle changes 2°. Within the CASSCF methodology, the distance N4–Cl6 is 0.066 Å larger when it is calculated with the (8, 8) active space than when the calculation is made by using the (6, 8) active space, and the rest of the bond lengths vary less than 0.02 Å. The maximum discrepancy in the bond and dihedral angles within the CASSCF calculations as a result of the choice of active space is only 1.1°, corresponding to the H5–N4–Cl6 bond angle.

Table 1. Geometrical parameters for I in its singlet state. Distances in angstroms and angles in degrees

	B3LYP/6-31G*	B3LYP/6-311 + G*	CASSCF(6, 8)	CASSCF(8, 8)
r(C1–N4)	1.454	1.458	1.460	1.462
r(N4–Cl6)	1.873	1.844	1.763	1.829
r(C1–C7)	1.596	1.584	1.563	1.563
r(C7–O8)	1.259	1.255	1.258	1.260
r(C7–O9)	1.243	1.243	1.230	1.230
∠(C1–N4–H5)	102.01	104.21	105.23	104.90
∠(C1–N4–Cl6)	112.21	112.05	112.64	111.74
∠(H5–N4–Cl6)	101.71	102.78	104.80	103.07
∠(N4–C1–C7)	106.83	108.26	109.14	109.27
∠(O8–C7–O9)	131.37	130.64	130.43	130.64
τ(C16–N4–C1–C7)	− 144.93	− 147.31	− 146.90	− 146.41

Table 2. Geometrical parameters for the TS in its singlet state

	B3LYP/6-31G*	B3LYP/6-311+G*	CASSCF(6, 8)	CASSCF(8, 8)
r(C1–N4)	1.379	1.367	1.346	1.352
r(N4–Cl6)	2.157	2.192	2.257	2.247
r(C1–C7)	1.760	1.799	1.921	1.835
r(C7–O8)	1.231	1.220	1.195	1.203
r(C7–O9)	1.227	1.219	1.190	1.208
∠(C1–N4–H5)	106.17	108.04	109.54	109.01
∠(C1–N4–Cl6)	112.25	112.24	112.05	112.05
∠(H5–N4–Cl6)	91.04	90.24	86.73	87.98
∠(N4–C1–C7)	103.96	103.71	98.93	100.29
∠(O8–C7–O9)	137.76	138.96	142.55	139.92
τ(C16–N4–C1–C7)	− 155.40	− 158.91	− 161.16	− 161.07

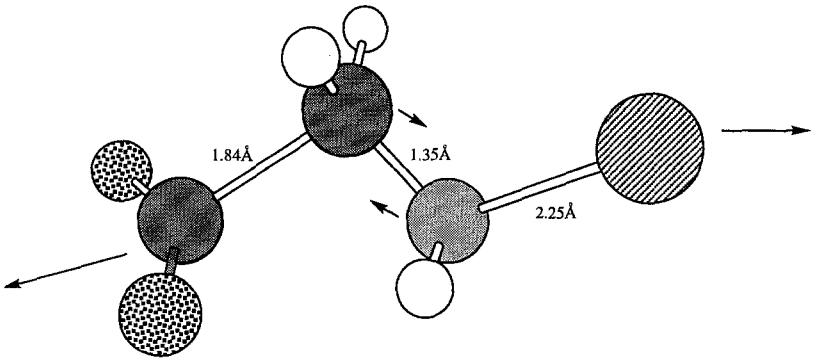

Fig. 2. TS for the decomposition process of the anionic form of N–Cl-α-glycine in its fundamental singlet state, calculated at the CASSCF(8,8)/6-31G* theoretical level. Arrows indicate the main atom motions corresponding to the imaginary frequency

The TS geometry (see Table 2) is found to be slightly changed when diffuse functions are included at DFT level, mainly in the N4–Cl6 and C1–C7 bond lengths (0.04 Å), in the C1–N4–H5 bond angle (2°), and in the Cl6–N4–C1–C7 dihedral angle (4°). CASSCF(8, 8) TS geometry in the singlet state is depicted in Fig. 2. When both (6, 8) and (8, 8) active spaces are compared, the C1–N4 and N4–Cl6 bond distances vary 0.01 Å and the largest change in bond lengths is found on the C1–C7 bond; this value fluctuates between 1.835 Å (8, 8) and 1.921 Å (6, 8). All changes in the angles are limited to variations of less than 1°, except for the O8–C7–O9 bond angle which ranges between 140° and 142.5°. When comparing DFT and CASSCF results small differences are found, mainly on the N4–Cl6 and C1–C7 bond lengths and also on the bond and dihedral angles.

It can be seen that all TSs have an antiperiplanar conformation of chlorine center Cl6 with respect to the carboxylate group, the C7–C1–N4–Cl6 dihedral angle ranging between 159° and 162° depending on the calculation level. As can be expected these values are increased with respect to those of I. This change in the geometry provides a greater overlap of π-orbitals at TS to yield the C1–N4 double bond formation.

3.2 Energies and activation parameters

The energies along with the activation parameters obtained for stationary points, I and TS, on the singlet and triplet surfaces are reported in Tables 3 and 4, respectively. When comparing between different methodologies a wide range of results for the barrier height are found: from 46 kcal/mol with the CASSCF(6, 8) level down to 1.62 kcal/mol with the B3LYP/6-31G* level in the singlet state, and from 44 kcal/mol with the CASSCF(8, 8) level to 2 kcal/mol with the B3LYP/6-311+G* level in the triplet state.

As can be seen, the calculations based on DFT yield very low values, 1.6–3.5 kcal/mol, for the barrier height in the singlet state. This trend has been recently noticed by our group in several studies of different chemical processes (like, for instance, the transposition of the α-chlorocyclobutanone or the unimolecular decomposition of several carboxylic acids derivatives, results to be published), i.e.,

Table 3. Calculated energy and thermochemical kinetics data in singlet state. Relative electronic energy (of the TS with respect to I) (ΔE_{el}) in kcal/mol. Activation enthalpy (ΔH)[a] in kcal/mol and activation entropy in cal/(mol K). All thermochemical values calculated at $T = 298.15$ K

Levels of calculation	ΔE_{el}	ΔS^a	ΔH^a
B3LYP/6-31G*	1.62	0.11	~0
B3LYP/6-311+G*	3.45	1.00	3.83
CASSCF(6, 8)/6-31G*	45.87	3.31	44.57
CASSCF(8, 8)/6-31G*	30.73	2.20	30.08
QCISD(T)/6-31G*	10.10	–	–

Table 4. Calculated energy data for the triplet state. The energy difference between the corresponding stationary points in triplet and singlet states are presented in parentheses. All values in kcal/mol

Levels of calculation	Relative electronic energy	
	I	TS
QCISD(T)/6-31G*	0.0 (32.44)	20.93 (43.26)
B3LYP/6-31G*	0.0 (22.47)	2.79 (23.63)
B3LYP/6-311+G*	0.0 (23.42)	2.14 (22.11)
CASSCF(8,8)	0.0 (111.68)	43.80 (130.37)

the energy profile is systematically smoothed by DFT methods with respect to the results obtained by standard HF or multiconfigurational schemes. This fact points out that, although the geometries of the stationary points and the transition vectors (TV) associated to TSs are described within the DFT methodology in a similar way than within standard calculation schemes, the energy values obtained must be taken with care and it is not obvious that DFT is appropriate in this respect.

It can also be seen that the relative electronic energy also changes depending on the active space size. The change from the (6, 8) active space to the (8, 8) implies a change in the relative energy from 45.87 to 30.73 kcal/mol in the singlet state. This change is expected, because it is well known that the CASSCF calculations are very sensitive to the choice of the active space.

The barrier height obtained with inclusion of correlation energy at the QCISD(T)/6-31G*//MP2/6-31G* level (10.10 kcal/mol) is very similar to the previously reported barrier height obtained at the MP2/6-31G* level in its singlet state (11.32 kcal/mol) [14]. On the other hand, a large difference is obtained for the triplet state (20.93 against 41.27 kcal/mol, respectively), although the general trend, i.e., the barrier height is higher for the triplet state, is maintained.

As can be seen, the singlet state has lower energy than the triplet in all stationary points. The energy difference between both states has a value of 112 kcal/mol at the reactant zone and 130 kcal/mol at the TS zone at CASSCF(8, 8) methodology while DFT renders values around 22–23 kcal/mol. If we compare the results with and without [15] electron correlation, we can observe that the inclusion of electron correlation increases the energy difference between the singlet and triplet electronic states. Due to this fact, complete optimization of

the stationary points on the first excited triplet state with the QCISD(T) and CASSCF levels has not been carried out. Keeping in mind these important differences between both surfaces we can state that the mechanistic path in gas phase is developed via the fundamental singlet state in accordance to our previous theoretical work [15].

The activation parameters calculated for the unimolecular decomposition of I in its singlet state are given in Table 3. The positive activation entropy (ranging from 0.11 to 3.31 cal/(mol K) is due to the fact that the reaction under study is a unimolecular decomposition process. Due to the variations found in the relative electronic energy, there are significant differences in the calculated activation enthalpy.

3.3 Normal mode and bond order analysis

The calculations of second derivatives of the total energy as predicted by various quantum mechanical methods are necessary in performing harmonic vibrational analyses and in particular to obtain the TV [47] associated to the TS. The imaginary frequency, and corresponding components of the eigenvector in the control space have been listed in Table 5 for the TS in its singlet state. As can be seen, there are two dominant contributions, as shown by a perusal of the amplitudes of the TV, i.e., the two bonds, C1–C7 and N4–Cl6, that are being broken. The TS is well associated in all cases to the decomposition process. The C1–N4 bond distance, which evolves from single to double bond, has minor participation in the TV. Together with these three distanaces, the TV components are associated to the C1–C7–O8 and C1–C7–O9 bond angles. The imaginary frequency values are in a wide interval, 173.8i–2495.9i cm^{-1}. DFT results present the lowest values, rendering a very smooth region around TS, in accordance with the previously commented characteristic of these methods (see above), while the CASSCF method presents higher values, in the range of 1915.5i–2495.9i.

The course of the reaction pathway can be studied by using a More O'Ferrall–Jencks [48, 49] diagram in terms of C1–C7 vs. N4–Cl6 bond orders; a schematic representation is given in Fig. 3. In our previous study [15], it was stated that the decomposition can be described as an asynchronous concerted process in gas phase, with no participation of the nitroniumlike or carbanionlike intermediates due to their non-existence on the PES as stationary points. The calculations reported in this paper confirm our early conclusion: we have not found stationary points corresponding either to those intermediates or to TSs that could

Table 5. Imaginary frequency (cm^{-1}) obtained from a normal mode analysis, and Hessian eigenvector components (*C*) for the TS in the singlet state

Imaginary frequency	B3LYP/6-31G* 173.7i	B3LYP/6-311+G* 232.2i	CASSCF(6,8) 1915.5i	CASSCF(8,8) 2495.9i
Parameters	*C*	*C*	*C*	*C*
r(C1–N4)	−0.14	−0.17	−0.24	−0.19
r(N4–Cl6)	0.67	0.67	0.70	0.46
r(C1–C7)	0.59	0.60	0.54	0.66
∠(C1–C7–O8)	−0.07	−0.08	−0.18	−0.12
∠(C1–C7–O9)	−0.13	−0.13	−0.16	−0.15

link the reactants to the putative intermediates. Furthermore, calculations at the CASSCF(8, 8)/6-31G*//HF/6-31G* level have been carried out in order to estimate the relative energy of the zone on PES corresponding to these hypothetical nitroniumlike and carbanion-like species, and values of 37 and 67 kcal/mol have been obtained, respectively. Thus, motion through a stepwise mechanism from the reactants to the upper-left or lower-right corners, representing carbanion-like or nitronium-like species, can be discarded in gas phase according to our results.

In order to calculate the progress of the decomposition process at the TS, Pauling bond orders [16] (BO) were calculated for TSs. Calculated BO in forming (C1–N4 and N4–Cl6 bonds) and breaking (C1–C7 bond) percentages are reported in Table 6. The different results obtained for the breaking/making bonds in all cases

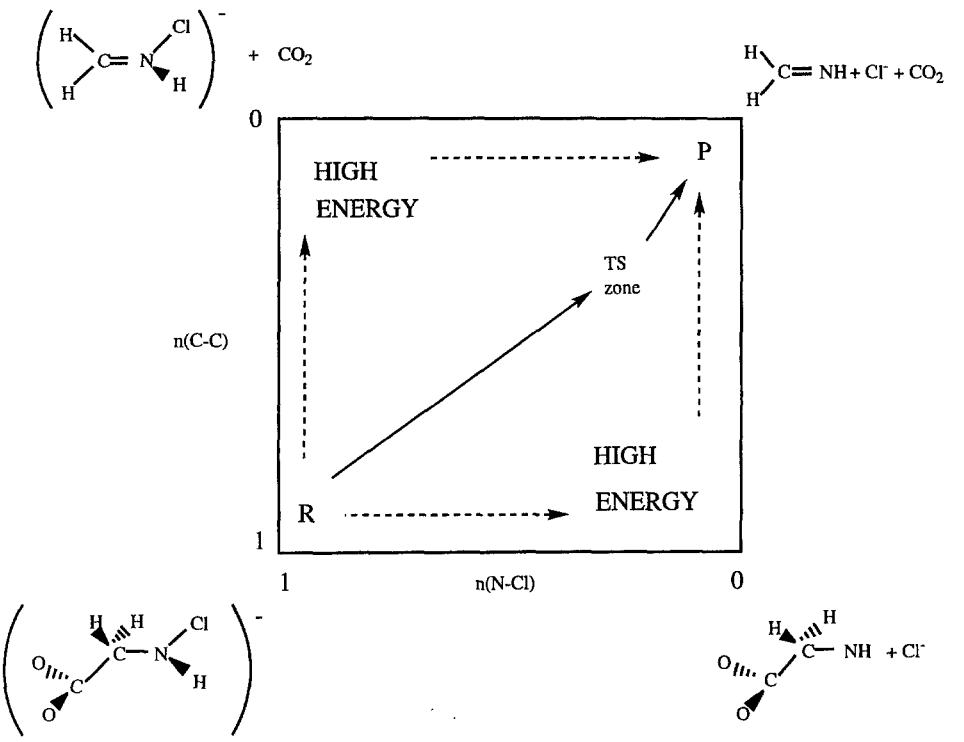

Fig. 3. A schematic respresentation by means of a More O'Ferrall–Jencks diagram for C1–C7 vs. N4–Cl6 breaking bond orders of the PES. Stationary points (R, TS, P) and hypothetical (nitroniumlike and carbanionlike species) minima are depicted

Table 6. Percentage of bond breaking at TS for equilibrium length of C1–C7 and N4–Cl6 bonds and percentage of bond making for eqilibrium length of C1–N4 double bond

	B3LYP/6-31G*	B3LYP/6-311+G*	CASSCF(6, 8)	CASSCF(8, 8)
r(C1–N4)	65.2	67.8	72.74	71.13
r(N4–Cl6)	61.1	68.7	80.71	75.19
r(C1–C7)	42.1	51.3	69.72	59.71

demonstrate the asynchronicity of the reaction. At the TS, the evolution of the bond cleavage and formation is advanced and the TS is product-like in all cases (see Fig. 3). This is in agreement with previous experimental and theoretical work [15, 50, 51]. However, some differences are located on the DFT results, yielding a minor product-like character for the three parameters and an early TS is found. These results can explain partially the low values of energy barriers found within the calculation methods based on DFT.

4 Conclusions

We present calculations by means of QCISD(T), DFT procedure at B3LYP/6-31G* and B3LYP/6-311 + G* levels, and MCSCF calculations in the (6, 8) and (8, 8) active spaces with the 6-31G* basis set, of equilibrium reactants and TSs relevant to molecular mechanism for the unimolecular decomposition of the anionic form of N-chloro-α-glycine in its singlet and triplet electronic states. The relevance of the present results can be summarized as follows:

(i) The energy of the PES for the triplet electronic state is higher than the energy for the PES of the singlet electronic state. The inclusion of electron correlation or the use of a multireference wave function increases this effect and by comparison with previous calculations, it is shown that the barrier heights are significantly affected. In spite of this, the main conclusion remains, i.e., the decomposition process is developed via the singlet electronic state in gas phase.
(ii) The detailed analysis of the PES demonstrates that decomposition is a concerted process in which the possible intermediates, i.e., carbanion and nitronium-like species, are not stationary points. An analysis of Pauling bond orders shows that the process is slightly asynchronous. The TSs are located in an advanced position along the reaction pathway, rendering a product-like character in agreement with experimental data.
(iii) Electron correlation effects basically modify the relative energies of TSs, meanwhile the geometry and unimolecular mechanism are qualitatively independent of the computing method.
(iv) It seems reasonable to assume that more studies should be conducted to verify our results incorporating solvent effects. This is presently being investigated and will be reported elsewhere.

Acknowledgments. This work was supported by Ministerio de Educación y Ciencia of Spanish Government by DGICYT (Project PB93-0661). All calculations were performed on a SGI POWER CHALLENGE L located at the Servei d'Informàtica of the Jaume I University. We are greatly indebted to this center for providing us computer facilities.

References

1. Owusu-Yaw J, Wheeler WB, Wei CI (1990) In: Water chlorination (Environmental Science and Technology). Lewis Publishers, Boca Raton, FL, vol 6, p 179
2. Franzén R, Kronberg L (1994) Environ Sci Technol 28:2222
3. Schonberg A, Moulbacher R (1952) Chem Rev 50:261
4. Stambro WD, Smith WD (1979) Environ Sci Technol 13:446
5. Friedman AH, Morgulis S (1936) J Am Chem Soc 58:909
6. Ingols RS, Wyckoff HA, Kethley TW, Hasdgen HW, Fincher EL, Webrand JC, Mandl JE (1953) Indus Eng Chem 45:996

7. Hand VC, Snyder MP, Margerum DW (1983) J Am Chem Soc 105:4022
8. Antelo JM, Arce F, Franco J, Rodriguez P, Varela A (1988) Int J Chem Kinet 20:433
9. Awad R, Hussain A, Crooks PA (1990) J Chem Soc Perkin Trans 2: 1233
10. Antelo JM, Arce F, Crugeiras J, Franco J, Varela A (1990) Int J Chem Kinet 22:1271
11. Armesto XL, Canle M, Losada M, Santaballa JA (1993) Int J Chem Kinet 25:1
12. Armesto XL, Canle M, Losada M, Santaballa JA (1993) Int J Chem Kinet 25:331
13. Armesto XL, Canle M, Losada M, Santaballa JA (1994) J Org Chem 59:4659
14. Ogata Y, Kimura M, Kondo Y (1981) Bull Chem Soc Japan 54:2057
15. Andrés J, Queralt JJ, Safont VS, Canle M, Santaballa JA (1996) J Phys Chem 100:3561
16. Pauling L (1947) J Am Chem Soc 69:542
17. Sosa CP, Andzelm J, Elkin BC, Wimmer E, Dobbs KD, Dixon DA (1992) J Phys Chem 96:6630
18. Berces A, Ziegler T (1993) J Chem Phys 98:4793
19. Handy NC, Murray CW, Amos RD (1993) J Phys Chem 97:4392
20. Seminario JM (1993) Chem Phys Letters 206:547
21. Johnson BG, Gill PMW, Pople JA (1993) J Chem Phys 98:5612
22. Estrin DA, Paglieri L, Corongiu G (1994) J Phys Chem 98:5653
23. Carpenter JE, Sosa CP (1994) J. Mol Struct (Theochem) 311:325
24. Gaussian94 (Revision A.1.), Frisch MJ, Trucks GW, Schlegel HB, Gill PMW, Johnson BG, Robb MA, Cheeseman JR, Keith TA, Petersson GA, Montgomery JA, Raghavachari MA, Al-Laham MA, Zakrzewski VG, Ortiz JV, Foresman JB, Cioslowski J, Stefanov BB, Nanayakkara A, Challacombe M, Peng CY, Ayala PY, Chen W, Wong MW, Andrés JL, Replogle ES, Gomperts R, Martin RL, Fox DJ, Binkley JS, Defrees DJ, Baker J, Stewart JP, Head-Gordon M, Gonzalez C, Pople JA (1995) Gaussian Inc., Pittsburgh, PA
25. Pople JA, Head-Gordon M, Raghavachary K (1987) J Chem Phys 87:5968
26. Hariharan PC, Pople JA (1973) Theoret Chim Acta 28:213
27. Wachters AJH (1970) J Chem Phys 52:1033
28. Hay PJ (1977) J Chem Phys 66:4377
29. McLean AD, Chandler GS (1980) J Chem Phys 72:5639
30. Krishnan R, Binkley JS, Seeger R, Pople JA (1980) J Chem Phys 72:650
31. Clark T, Chandrasekhar J, Spitznagel GW, Schleyer PvR (1983) J Comp Chem 4:294
32. Frisch MJ, Pople JA, Binkley JS (1984) J Chem Phys 80:3265
33. Raghavachari K, Trucks GW (1989) J Chem Phys 91:1062
34. Andzelm J, Wimmer E (1992) J Chem Phys 96:1280
35. Sim F, St-Amant A, Papai I, Salahub DR (1991) J Am Chem Soc 114:4391
36. Gill PMW, Johnson BG, Popleand JA, Frisch MJ (1992) Chem Phys Lett 197:499
37. Lee C, Yang W, Parr RG (1988) Phys Rev B 37:785
38. Miehlich B, Savin B, Stoll H, Preuss H (1989) Chem Phys Lett 157:200
39. Becke AD (1993) J Chem Phys 98:5648
40. Roos BO (1987) Adv Chem Phys 69:399
41. Schlegel HB (1982) J Comp Chem 3:214
42. Schlegel HB (1982) J Chem Phys 77:3676
43. Baker J (1986) J Comp Chem 7:385
44. Baker J (1987) J Comp Chem 8:563
45. Grev RS, Janssen CL, Schaefer III HF (1991) J Chem Phys 95:5128
46. McQuarrie DA (1986) Statistical mechanics. Harper & Row, New York
47. Stanton RW, McIver Jr JV (1975) J Am Chem Soc 97:3632
48. More O'Ferrall RA (1970) J Chem Soc B 274
49. Jencks WP (1972) Chem Rev 72:705
50. Canle M (1994) PhD Thesis, Universidad de La Coruña, Spain
51. Andrés J, Queralt JJ, Safont VS, Canle M, Santaballa JA (1996) J Phys Org Chem 9:371